Chemical Engineering Journal 147 (2009) 219–225

Contents lists available at ScienceDirect

Chemical Engineering Journal

journal homepage: www.elsevier.com/locate/cej

The effect of Praseodymium on the adsorption and photocatalytic degradation of azo dye in aqueous Pr^{3+}-TiO_2 suspension

Chunhua Liang[a,*], Chengshuai Liu[b], Fangbai Li[b], Feng Wu[a]

[a] Department of Chemistry, Huaihua University, Huaihua, Hunan 418008, China
[b] Guangdong Key Laboratory of Agro-Environment Pollution Integrated Control, Guangdong Institute of Eco-Environment and Soil Sciences, Guangzhou 510650, China

ARTICLE INFO

Article history:
Received 24 April 2008
Received in revised form 25 June 2008
Accepted 1 July 2008

Keywords:
Praseodymium
Photocatalysis
Azo dye
Ion doping
TiO_2

ABSTRACT

Praseodymium ion-doped TiO_2 (Pr^{3+}-TiO_2) were prepared by the sol–gel method. The catalysts were characterized structurally by X-ray diffraction (XRD) and diffusive reflectance spectra (DRS) methods. The XRD results show that doped Pr ion could stabilize the anatase phase of TiO_2 and also inhibit the increase of the crystallite size. The DRS results show that the optical absorption edge slightly shifted to red direction owing to praseodymium ion doping, and Pr^{3+} doped TiO_2 (Pr^{3+}-TiO_2) catalysts had higher absorption peaks in the ultraviolet region. Pr^{3+}-TiO_2 had better adsorption capacities and photocatalytic abilities for dye removal than that of pure TiO_2. The optimum proportion of doped Pr ion for degradation of azo dye was 1.5% under UV light and 1.0% under visible light, at which best for dye photocatalytic degradation. The red shift of the optical adsorption edge of TiO_2 and visible light adsorption by Pr^{3+} doping were the key factors that enhanced the photocatalytic activity of the catalysts when irradiated with visible light.

1. Introduction

Reactive yellow, one group of azo dyes, has wide applications in coloring paper, temporary hair colorant, dyeing cottons, and wools, especially dye finishing process [1]. Although not most high hazardous, azo dyes can cause some harmful effects, such as heartbeat increase, vomiting, shock, cyanosis, jaundice, quadriplegia, and tissue necrosis in humans [2–4]. Efficient removal of azo dyes from wastewater is a critical problem since even a small amount of dye is clearly apparent. In the past decades, techniques such as adsorption, combustion, wet oxidation and so on, had been studied to degrade azo dyes. However, the low mineralization efficiency and high cost effectiveness of these techniques limited the application in the practical wastewater treatment process [5,6].

Heterogeneous photocatalysis is one of the most important efficient technologies used for removal of organic contaminants from wastewater. Photocatalytic processes with TiO_2 are preferred studies in the past years due to several reasons such as: (i) complete mineralization; (ii) no waste disposal problems; (iii) no expensive oxidants needed; (iv) low costs; (v) only mild temperature and pressure are necessary [6–9]. However, since its large band-gap energy (E_g = 3.2 eV) considerably limits the utilization of natural solar light or artificial visible light, TiO_2 photocatalyst has not been applied widely in the field of environmental pollution control. Traditional visible light responsive catalysts either are unstable under illumination (such as CdS and CdSe) or have low activity (such as WO_3 and Fe_2O_3) [10]. Modification of TiO_2 to extend its absorption edge toward the visible light region has been the subject of recent research [11,12]. Among different modification methods, doping with rare earth ions or their oxides is an effective method [13,14]. Rare earth ions have strong complex ability to adsorb various organic pollutants and facilitate the decolorization of dyes [15,16]. Moreover, TiO_2 doping with rare earth ions can reduce the crystallite size and increase the surface area of TiO_2, which also causes the enhancement of adsorption capacity of TiO_2 [17,18]. It has been reported that TiO_2 doping with rare earth ions can lead to red shift of absorption edge, which is one of the important ways to improve the photocatalytic activity of TiO_2 when irradiated with visible light [19]. The transitions of 4f electrons of rare earth ions can also improve photocatalytic activity of TiO_2 under both UV and visible light irradiation by increasing the separating rate of photogenerated charges [20–22]. Thus, it is suggested that rare earth doping can provide better adsorption abilities and better photocatalytic performances. To our knowledge, however, the doping of rare earth metals, particularly Pr^{3+}, in TiO_2, and their catalytic properties have seldom been presented so far, especially for the systemically studying of adsorption property and photocatalytic activities for azo dye degradation under both UV and visible light irradiation.

In this paper, we concentrate our research on adsorption properties and photocatalytic activity of Pr^{3+}-TiO_2, the less reported metal

* Corresponding author. Tel.: +86 745 2851014; fax: +86 745 2851305.
E-mail address: lchmyl@126.com (C. Liang).

1385-8947/$ – see front matter © 2008 Elsevier B.V. All rights reserved.
doi:10.1016/j.cej.2008.07.004

Table 1
Properties of RY-4

Parameter	RY-4
Commercial name	Reactive Yellow 4
Color	Brown yellow
Class	Reactive dye
Solvent	Water
Empirical formula	$C_{56}H_{38}Cl_2N_{14}O_{20}S_6{\cdot}6Na$
Formula weight	1628

ion-doped TiO_2 catalysts [23]. A series of Pr ion-doped titanium dioxide (Pr^{3+}-TiO_2) catalysts were prepared at different proportion by the sol–gel method. Reactive Yellow 4 (RY-4), one of reactive yellow dyes, was used as the model pollutant to investigate the mechanisms of increased adsorption and photodegradation activities of the Pr ion-doped TiO_2 (Pr^{3+}-TiO_2) catalysts under UV and visible light irradiation, respectively, in aqueous suspension.

2. Experimental

2.1. Materials

Reactive Yellow 4 (RY-4) used as received was purchased from the Special Chemical Corporation of Shanghai, China. All the other chemicals were purchased form Guangzhou Chemical Corporation, Guangzhou, China. The properties (name, color and molecular weight) of RY-4 and its chemical structure are shown in Table 1 and Fig. 1. The pure TiO_2 and Praseodymium ion-doped TiO_2 (Pr^{3+}-TiO_2) catalysts were prepared with the raw materials in analytical grade. The raw materials included tetra-*n*-butyl titanium [Ti(O-Bu)$_4$], Pr$(NO_3)_3$, acetic acid (99.8%), absolute ethanol and ethanol (95%). All the materials were used as received. Deionized water was used to prepare the solutions in the experiments.

2.2. Preparation of Pr^{3+}-TiO_2 catalyst

Pr^{3+}-TiO_2 catalysts were prepared by a sol–gel process with the following procedure: firstly, 17 mL of tetra-*n*-butyl titanium (Ti(O-Bu)$_4$) was dissolved in 80 mL of absolute ethanol, secondly, the obtained Ti(O-Bu)$_4$ solution was added drop-wise under vigorous stirring into 100 mL of a mixture solution which contained 84 mL of ethanol (95%), 2.5 mL of 0.1 M Pr $(NO_3)_3$, and 15 mL of acetic acid (>99.8%), and then the resulting transparent colloidal suspension was stirred for 2 h before ageing for several days until formation of gel. In the third step, the gel was vacuum dried at 373 K and then ground. Finally, after being sintered at 773 K for 2 h, Pr^{3+}-TiO_2 catalysts were obtained. This Pr^{3+}-TiO_2 catalyst had a nominal atomic ratio (Pr/Ti) of 0.5%, so it is named as 0.5% Pr^{3+}-TiO_2 in this study. The other Pr^{3+}-TiO_2 samples containing different Praseodymium ion contents were prepared using the same procedure with different content of Pr$(NO_3)_3$, and the obtained catalysts were named accordingly as 1.0% Pr^{3+}-TiO_2, 1.5% Pr^{3+}-TiO_2, and 1.8% Pr^{3+}-TiO_2, respectively.

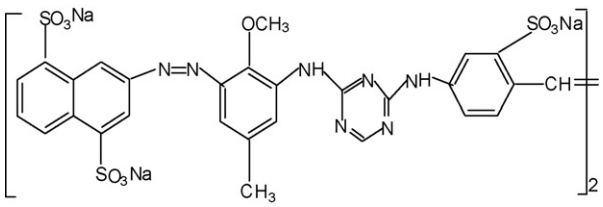

Fig. 1. Chemical structure of Reactive Yellow 4.

2.3. Characterization

To determine the crystal phase composition of the prepared TiO_2 and Pr^{3+}-TiO_2 samples, X-ray diffraction (XRD) characterization was carried out at room temperature using a Rigaku D/MAX-IIIA diffractometer with Cu Kα (λ = 0.15418 nm) with the accelerating voltage of 30 kV and the emission current of 30 mA. Diffuse reflectance spectra (DRS) of the catalyst in the wavelength range of 350–700 nm were obtained using a UV–vis spectrophotometer (Shimadzu UV-2101PC), with $BaSO_4$ as a reference.

2.4. Adsorption isotherm experiment

Adsorption is an indispensable step in any heterogeneous photocatalytic reaction. The adsorption behaviors of pure TiO_2 and Pr^{3+}-TiO_2 catalysts were investigated at first in this study. A fixed amount of Pr^{3+}-TiO_2 (0.1 g) was added into 10 mL of RY-4 solution with different concentrations, respectively, in the reactor of stoppered glass tubes. And then the reactors were shaken at 180 rpm in a thermostatic shaker bath at the constant temperature of 25 ± 1 °C for 24 h. At time t = 0 and 24 h, the RY-4 concentrations in the solutions were determined by UV–vis Spectrometer and the adsorbed amount of RY-4 on pure TiO_2 or Pr^{3+}-TiO_2 catalysts were calculated based on a mass balance.

2.5. Photo reactor system and experimental procedures

A Pyrex cylindrical photo reactor (as seen in Fig. 2) was used in the experiments, in which an 8-W medium-pressure mercury lamp with an emission peak at 365 nm (Westbury, New York) or a 70 W high-pressure sodium lamp (Shanghai, China) with main emission in the range of 400–800 nm was positioned at the centre of the cylindrical vessel and surrounded by a circulating water jacket to control the temperature at 25 ± 1 °C during reaction. The reaction suspension was prepared by adding 0.25 g of photocatalyst powder into 250 mL of aqueous RY-4 solution. Prior to photocatalytic oxidation, the suspension was magnetically stirred in a dark condition for 30 min to establish adsorption/desorption equilibrium. The aqueous suspension containing RY-4 and photocatalyst was irradiated under UV or Vis illumination with constant aeration. At the given time intervals, the 10 mL of samples were taken from the suspension and immediately centrifuged at 4500 rpm for 20 min, then filtered through a 0.45 μm Millipore filter to remove the particles. The filtrate was stored in the dark for needed analysis.

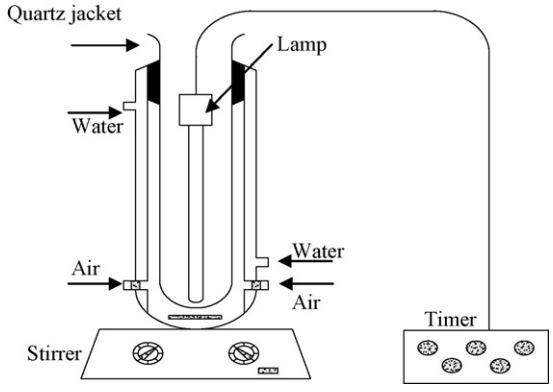

Fig. 2. Scheme of the photocatalytic reactor for photocatalytic degradation of RY-4.

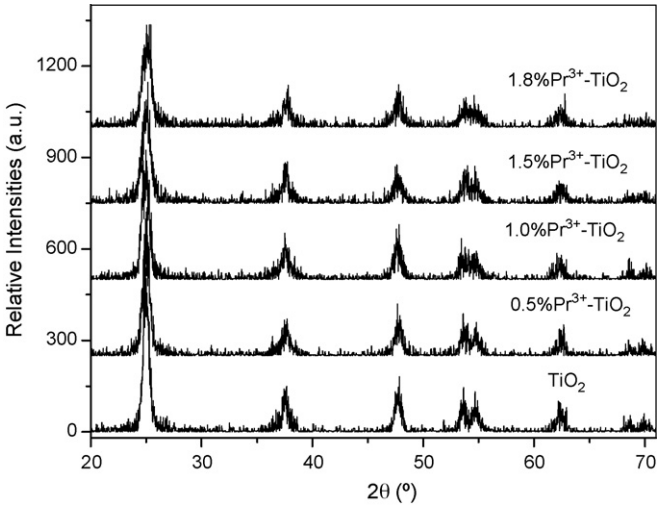

Fig. 3. The XRD patterns of TiO_2 and Pr^{3+}-TiO_2 catalyst powders.

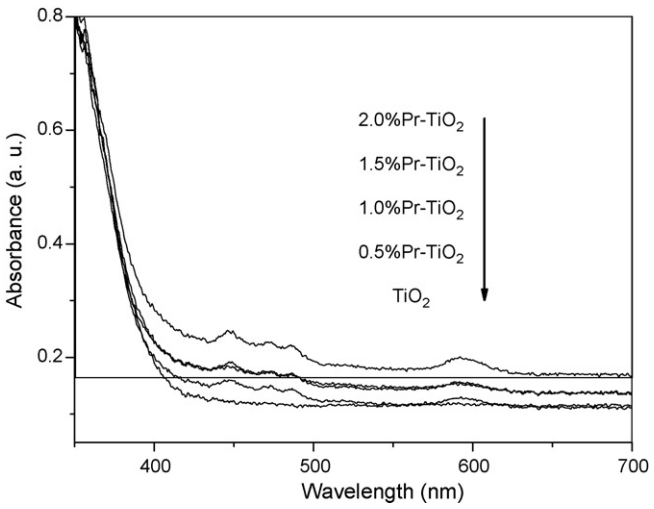

Fig. 4. The UV–vis diffuse reflectance spectra of TiO_2 and Pr^{3+}-TiO_2 catalysts.

2.6. Analytic method

To measure RY-4 concentration, UV–vis spectrophotometer (UV–vis TU-1800, Purkinje General, Beijing) was used to determine the absorbance of RY-4 at the wavelength of 417 nm. The total organic carbon (TOC) concentration was determined using a Total Organic Analyzer instrument (Shimadzu TOC-V CPH).

3. Results and discussion

3.1. X-ray diffraction analysis of catalysts

The XRD patterns of pure TiO_2 and Pr^{3+}-TiO_2 catalyst powders are presented in Fig. 3, which show that all catalysts are dominated by anatase TiO_2 and the relative intensity of (1 0 1) peak decrease significantly with increasing the dosage of Praseodymium ion. Based on the XRD data, the crystallite sizes of the Pr^{3+}-TiO_2 samples were calculated using the Scherrer Formula and the results show that the crystallite sizes decrease with increasing the Pr^{3+} content (Table 2). From Table 2, it can be also found that there is no obvious difference between the pure TiO_2 and Pr^{3+}-TiO_2 powders as to the lattice parameter '*a*' and '*c*', which indicate that rare earth ion doping can hinder the increase of the crystallite size [24].

3.2. Diffusive reflectance spectra analysis

To study the optical absorption properties of the catalysts, DRS in the range of 350–700 nm was investigated and the result is shown in Fig. 4, from which it can be seen that pure TiO_2 had no adsorption in the visible light region (>400 nm), while Pr^{3+}-TiO_2 catalysts have wide absorption band in the range of 400–600 nm. The wide spectral band in 400–500 nm was ascribed to the f→ f transition absorption. At around 600 nm a weak adsorption peak exists, which was ascribed to the characteristic transition of Pr^{3+} $^1D_2 \rightarrow {}^3H_4$ [25]. In addition, the optical absorption of Pr^{3+}-TiO_2 in the UV region was also enhanced. The transitions of 4f electrons of Pr^{3+} favored the separation of photo-generated electron–hole pairs, and also favored the sensitization of TiO_2 with visible light and the complexation with azo dyes. It can also be seen that there are red shifts of the optical adsorption edge of TiO_2 by Pr ion doping, which is helpful to improve the photocatalytic activity of TiO_2 when irradiated with visible light.

Table 2
Crystal parameters of different catalysts

	Pr^{3+} doping content (mol/mol)				
	0.0%	0.5%	1.0%	1.5%	1.8%
Stucture type	Anatase	Anatase	Anatase	Anatase	Anatase
Surface area (m^2/g)	78.44	96.47	105.81	109.79	108.29
Crystallite size (nm)	30.3	23.1	15.1	15.7	9.64
Lattice parameter *a* (nm)	0.380	0.380	0.382	0.381	0.379
Lattice parameter *c* (nm)	0.956	0.953	0.958	0.954	0.953
1 0 1 peak relative intensity (cps)	473	405	348	316	283

3.3. Absorption behavior

Adsorption of pollutants on the surface of semiconductor is an important factor in heterogeneous photocatalysis. A set of adsorption experiments were performed to determine the adsorption behavior of RY-4 on pure TiO_2 and Pr^{3+}-TiO_2 catalysts. As shown in Fig. 5a, RY-4 was adsorbed on Pr^{3+}-TiO_2 catalysts rapidly and the maximum capacity on the 1.8% Pr^{3+}-TiO_2 catalyst was 16.59×10^{-6} mol/g, which was much higher than on pure TiO_2 of 10.89×10^{-6} mol/g. The adsorption isotherms of RY-4 can be analyzed by Langmuir adsorption model:

$$\frac{C_e}{Q_e} = \frac{1}{Q_{max}K_a} + \frac{C_e}{Q_{max}} \quad (1)$$

where C_e is the concentration of the substrate in the solution at equilibrium (mol/L), Q_e is the adsorption amount in the solution at equilibrium (mol/g). K_a is the Langmuir adsorption equilibrium constant in mol/g. Q_{max} is the saturated adsorption amount.

The plot of C_e/Q_e versus C_e would give a straight line (Fig. 5b), and then Q_{max} and K_a can be derived from the intercept and the slope of the plot. The correlation coefficient R represents the conformity between the experimental results and the Langmuir adsorption isotherm model. According to the adsorption experimental data of RY-4 on different catalysts, K_a, Q_{max} and the correlation coefficient are obtained and presented in Table 3.

The results indicated that the values of adsorption equilibrium constants (K_a) of Pr^{3+}-TiO_2 catalysts are much higher than that of the pure TiO_2 catalyst and Q_{max} are also higher than that of the pure TiO_2 catalyst. The factors that led to the enhanced adsorption capacity should involve the change of the physical or chemical properties of the catalysts owing to Pr ion doping. The smaller crystal size and larger specific surface area of Pr^{3+}-TiO_2 catalysts would result in the

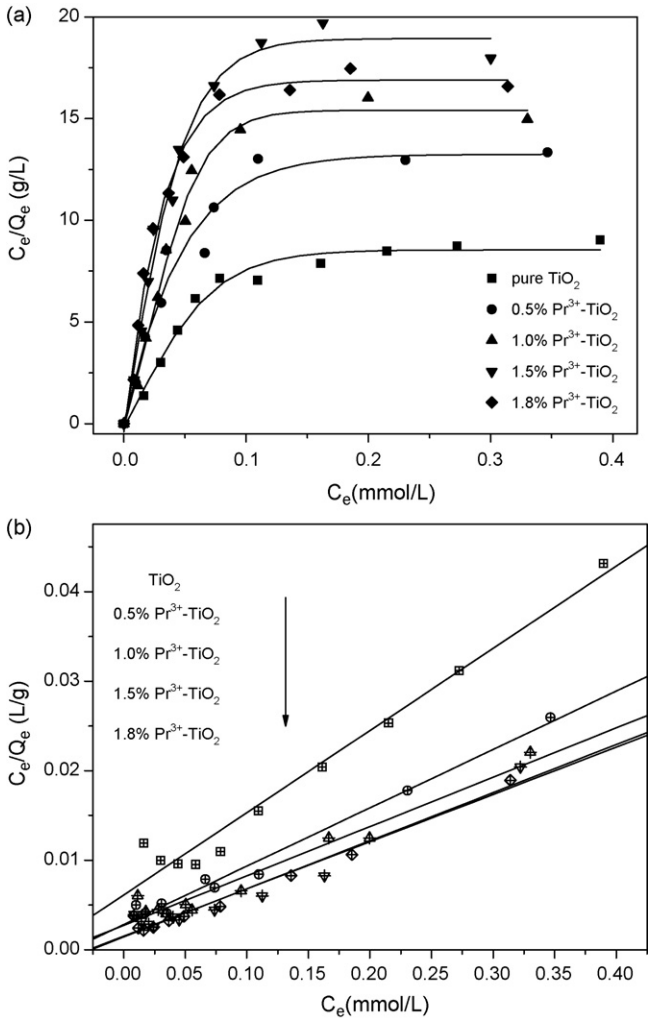

Fig. 5. Adsorption isotherms of RY-4 on pure TiO_2 and Pr^{3+}-TiO_2 catalyst.

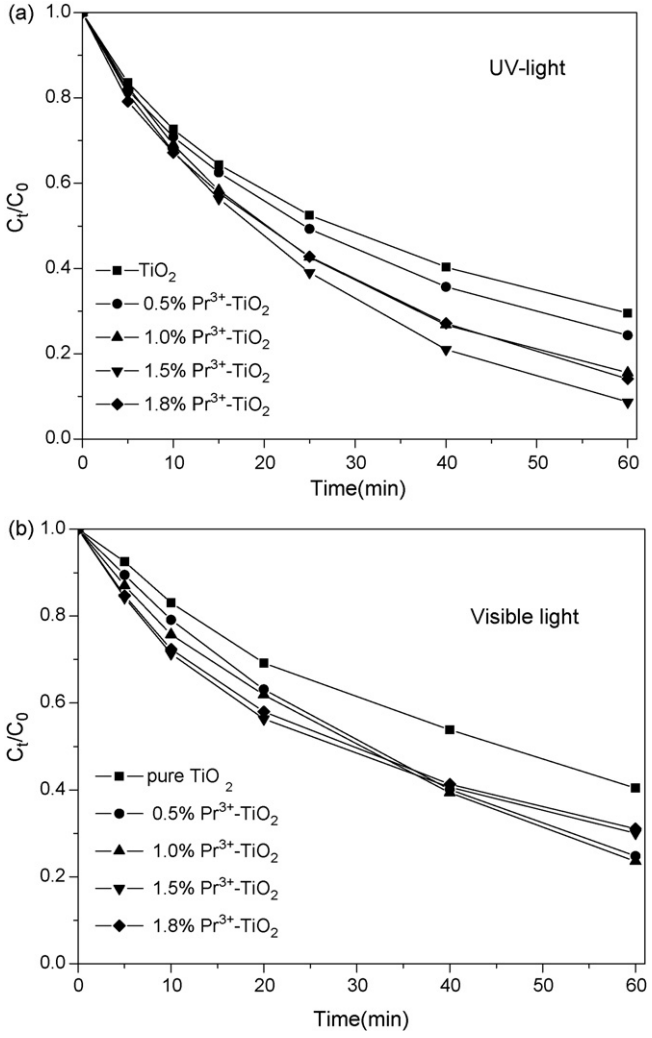

Fig. 6. The photocatalytic degradation of 6×10^{-5} mol/L RY-4 under UV light (a) and visible light irradiation (b) (pH 6.56, catalyst dosage: 1.0 g/L).

better physical adsorption of RY-4. Moreover, it was reported that Pr^{3+} and other lanthanide ions can complex with azo dyes to form solid complexes [23,26]. Thus, forming a chemical complex of Pr^{3+} and RY-4 might be another important enhancement mechanism for the adsorption of RY-4 on Pr^{3+}-TiO_2 in the aqueous suspension.

3.4. Photocatalytic activity of Pr^{3+}-TiO_2

To evaluate the effects of Pr ion dosage on the photocatalytic activity of catalysts, two sets of experiments of degrading RY-4 in aqueous suspensions under UV light and visible light, respectively, were conducted in this study. The degradation kinetics of RY-4 on different catalysts under UV light and visible light could be well analyzed by the pseudo-first-order kinetic model. The results of RY-4 degradation rate by different Pr^{3+}-TiO_2 were presented in Fig. 6 and the values of kinetic constants k_r and the correlation coefficient R^2 are listed in Table 4. It is shown that the photocatalytic activity of Pr ion-doped TiO_2 was significantly higher than that of pure TiO_2 under both UV light and visible light. Under light irradiation even of visible light, RY-4 can be excited and an excited electron is generated. Then the excited electron can be transformed to TiO_2, then to O_2, and $O_2^{\bullet -}$ and hydroxyl radical are generated, as described by following equations. Therefore pure TiO_2 should have photocatalytic activity owing to dye sensitization [27,28]. The photocatalytic activity of TiO_2-based catalysts increased with increasing the Pr^{3+} doping dosage initially, but decreased when Pr^{3+} doping content was over 1.5% under UV light and 1.5% under visible light. 1.5% Pr^{3+}-TiO_2 achieved the best photocatalytic performance under UV light and 1.0% Pr^{3+}-TiO_2 performed best under visible light. Under visible light, RY-4 can be excited and an excited electron is generated. Then the excited electron can be transformed to TiO_2, then

Table 3
Langmuir isotherm constants for adsorption of RY-4 on different catalyst

	Photocatalysts				
	TiO_2	0.5% Pr^{3+}-TiO_2	1.0% Pr^{3+}-TiO_2	1.5% Pr^{3+}-TiO_2	1.8% Pr^{3+}-TiO_2
K_a ($\times 10^3$ L/mol)	14.96	23.29	20.41	35.20	38.36
Q_{max} ($\times 10^{-6}$ mol/g)	10.89	18.15	18.94	18.62	16.59
R^2	0.973	0.984	0.950	0.942	0.977

Table 4
The data of pseudo-first-order rate of RY-4 under UV light and visible light

	Photocatalysts				
	TiO_2	0.5% Pr^{3+}-TiO_2	1.0% Pr^{3+}-TiO_2	1.5% Pr^{3+}-TiO_2	1.8% Pr^{3+}-TiO_2
K_r (min^{-1})					
UV light	0.0221	0.0251	0.0321	0.0399	0.0331
Visible light	0.0155	0.0231	0.0239	0.0216	0.0210
R^2					
UV light	0.958	0.974	0.994	0.998	0.995
Visible light	0.992	0.999	0.998	0.952	0.957

to O_2, and leading to the generation of $O_2^{\bullet -}$ and hydroxyl radical, as described by Eqs. (2)–(7). Therefore pure TiO_2 should have photocatalytic activity due to dye sensitization.

$$Dye + h\nu \rightarrow Dye^* \quad (2)$$

$$TiO_2 + Dye^* \rightarrow TiO_2(e^-) + Dye^{\bullet +} \quad (3)$$

$$O_2 + TiO_2(e^-) \rightarrow O_2^{\bullet -} + TiO_2 \quad (4)$$

$$O_2^{\bullet -} + H_2O \rightarrow HO_2^{\bullet} + OH^- \quad (5)$$

$$HO_2^{\bullet} + H_2O + TiO_2(e^-) \rightarrow H_2O_2 + OH^- + TiO_2 \quad (6)$$

$$H_2O_2 + TiO_2(e^-) - OH^{\bullet} + OH^- + TiO_2 \quad (7)$$

To describe the degradation kinetics of RY-4 in the aqueous suspension, the Langmuir–Hinshelwood (L–H) model was applied to deal with the experiment data. In fact, the L–H model was established based on Langmuir adsorption of the organic substrate onto the photocatalyst. Thus, the aspect of substrate adsorption was included in the L–H model [29]. The L–H model can be expressed as follows:

$$-\frac{dC}{dt} = k_r \frac{K_a C}{1 + K_a C} \quad (8)$$

where $-dC/dt$ is the photo-catalytic colorization rate in mol/(L min), k_r is the colorization reaction rate constant also in mol/(L min), t is reaction time in min, C is the concentration of RY-4 (mol/L), t is the time (min) and K_a is the Langmuir adsorption equilibrium constant (L/mol).

If the product of C and K_a is significantly smaller than 1, Eq. (8) may be simplified to pseudo-first-order kinetic equation as follows:

$$-\frac{dC}{dt} = k_r K_a C \quad (9)$$

Consequently an integrated form of Eq. (9) can be expressed as:

$$-\ln\left(\frac{C}{C_0}\right) = k_r K_a t \quad (10)$$

In this work, the initial concentration (C_0) of RY-4 was around 0.06×10^{-3} mol/L, the products of $K_a C_0$ were calculated to be between 0.898 and 2.30. Obviously, it should not be neglected compared to 1 in Eq. (10). Under this situation, an integral form of the L–H model would be more feasible, as expressed below:

$$\ln\left(\frac{C_0}{C}\right) + K_a(C_0 - C) = k_r K_a t \quad (11)$$

Eq. (11) can also be rearranged as follows:

$$\ln\left(\frac{C_0}{C}\right) + K_a(C_0 - C) = k_{ap} t \quad (12)$$

where $k_{ap} = k_r K_a$, is the apparent rate constant in 1/min. The k_{ap} value can be obtained by plotting $\ln(C_0/C) + K_a(C_0 - C)$ versus t.

The adsorption equilibrium coefficients (K_a) have been obtained in Section 3.3 which listed in Table 3, and the apparent rate constants (k_{ap}) can be obtained by plotting $\ln(C_0/C) + K_a(C_0 - C)$ versus t. Then the photoreaction kinetic constants (k_r) can be calculated by $k_{ap} = k_r K_a$. Under UV illumination, the apparent rate constant (k_{ap}) and the photoreaction kinetic constants (k_r) versus Pr ion doping amount is presented in Fig. 7. It can be seen that the photoreaction kinetic constants (k_r) did not change obviously, which suggest that adsorption plays an important role in the process of photocatalytic colorization of RY-4 by Pr^{3+}-TiO_2.

3.5. Mineralization of RY-4

Fig. 8 shows the TOC removal of RY-4 degradation after 120 min under UV light irradiation with different catalysts, which indicating the efficient mineralization of the azo dyes. The percentages of TOC removal are 61.9%, 72.7%, 82.8%, 69.2%, and 59.3% when in the suspension of pure TiO_2, and 0.5%, 1.0%, 1.5%, and 1.8% Pr^{3+}-TiO_2, respectively. The percentage of TOC removal of TiO_2 based catalysts increased with increasing the Pr^{3+} doping dosage initially, but decreased when Pr^{3+} content was over 1.0%. Obviously,

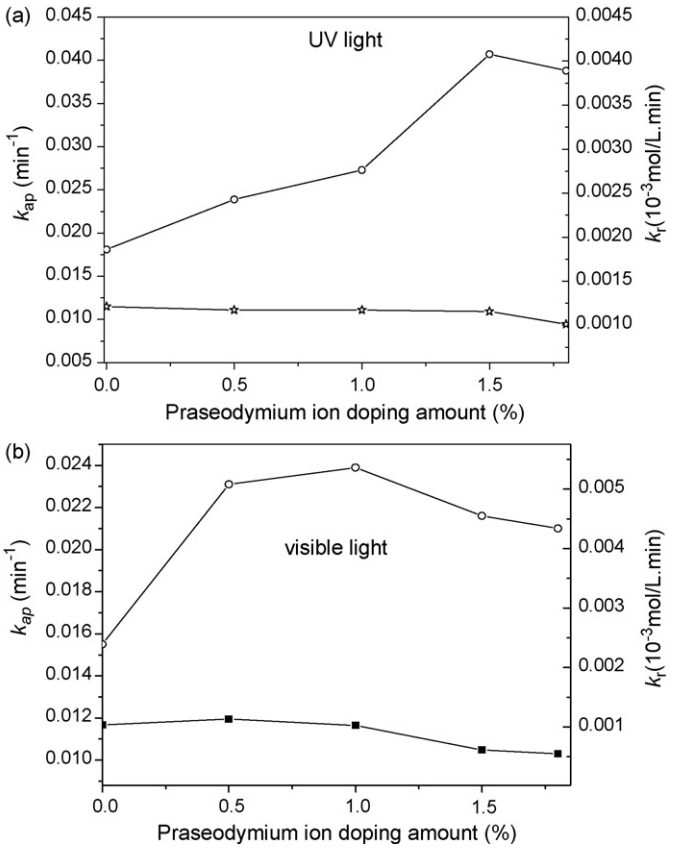

Fig. 7. Apparent kinetic constant (k_{ap}) and kinetic constant (k_r) of RY-4 photocatalytic degradation by using Pr^{3+}-TiO_2 catalyst under: (a) UV light and (b) visible light irradiation.

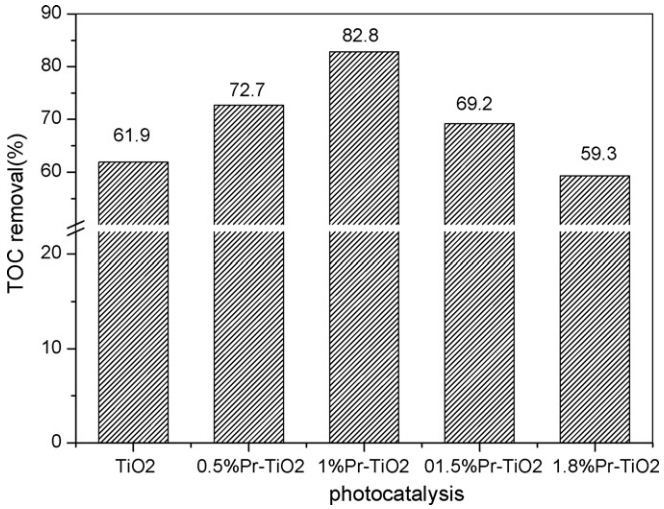

Fig. 8. TOC removal percentage of 6×10^{-5} mol/L RY-4 solution using 1.0 g/L different photocatalysts after 120 min under UV light irradiation.

1.0% Pr^{3+}-TiO_2 had the best performance for TOC removal, which was not consistent with that of the photocatalytic activity for RY-4 degradation, because TOC removal was attributable to the mineralization of RY-4, while the photocatalytic degradation for RY-4 was attributable to the decolorization due to the breakage of –N=N– in the molecular of RY-4.

4. Discussions

The DRS spectra of Pr^{3+}-doped TiO_2 catalysts show that slightly red shifts occurred and there were optical adsorption in visible region in the doped catalysts, owing to the transitions of 4f electrons of Pr^{3+} from $^4I_{15/2}$ to $^4F_{7/2}$, $^2H_{11/2}$ and $^4F_{9/2}$. The transitions of 4f electrons of Pr^{3+} favored the formation of photogenerated electron–hole pairs. And also, the incorporation of Pr ions into the TiO_2 nanoparticles prepared by sol–gel method can also result in the red shift due to the charge-transfer transitions between the Pr ion electrons and the TiO_2 conduction or valence band [30].

It is well known that the high photocatalytic activity of photocatalysts was ascribed to both of the better adsorption of organic substrate and the improvement of the interfacial charge-transfer reaction. And also, it has been concluded that the larger surface area from the above results because of the smaller particle size [24]. So, as mentioned above in this study, the small crystallite size and the Pr^{3+} complex effect of the Pr^{3+}-TiO_2 catalysts are favorable for the better adsorption of RY-4, which result in the high activity for RY-4 degradation. Furthermore, it has been reported that the pairing effect of the ion doping could result in the appearance of a solid solution in Pr^{3+}-doped TiO_2 sol–gel layer [31]. So, Pr ion doping might be more favorable for the separation of photoinduced electron–hole pairs, which lead to the enhancement of photocatalytic activity [32].

The optimal dosage of Pr ion doping of 1.5% under UV irradiation may be due to the fact that there was an optimal dosage of Pr ions in TiO_2 particles most favorable for separation of photoinduced electron–hole pairs. With increasing the dosage of doped Pr^{3+}, the surface barrier of Pr^{3+}-TiO_2 becomes higher, resulting in the narrower space charge region. So the electron–hole pairs within the region are efficiently separated by the large electric field. Moreover, when the concentration of doped ions is excessively high, the space charge region becomes very narrow and the penetration depth of light into TiO_2 exceeds the space charge layer greatly, so, the recombination of the photo generated electron–hole pairs becomes easier, which leading to the decreased degradation of RY-4. Thus, the optimum Pr^{3+} doping for degradation of RY-4 was existed in Pr^{3+}-TiO_2 photocatalysts.

5. Conclusions

Pr ion doping could thermally stabilize anatase phase of TiO_2 and inhibit the increase of the crystallite size, and also, can improve the adsorption of RY-4 significantly. The degradation rates of RY-4 under UV light and visible light radiation were higher with Pr^{3+}-TiO_2 catalyst than those with pure TiO_2, and the optimal dosage of Pr ion was 1.5% and 1.0% when irradiated with UV and visible light, respectively. Pr^{3+}-TiO_2 could mineralize RY-4 more efficiently than pure TiO_2. The separation efficiency of interfacial charges by Pr^{3+} doping may lead to an optimal Pr^{3+} dosage for the degradation of RY-4. The transitions of 4f electrons of Pr^{3+} and the red shift of the optical absorption edge of TiO_2 by Pr^{3+} doping were important for enhancing photocatalytic activity under visible light.

Acknowledgements

The authors wish to thank the Technological Foundation of Guangdong Province (2005B10301001) and the Scientific Research Foundation of Huaihua University for financial supports to this work.

References

[1] M. Koch, A. Yediler, D. Lienert, G. Insel, A. Kettrup, Ozonation of hydrolyzed azo dye reactive yellow 84 (CI), Chemosphere 46 (2002) 109–113.
[2] M.R. Hoffmann, S.T. Martin, W. Choi, D.W. Bahnemann, Environmental applications of semiconductor photocatalysis, Chem. Rev. 95 (1995) 69–96.
[3] S.B. Bukallah, M.A. Rauf, S.S. Ashraf, Photocatalytic decoloration of Coomassie Brilliant Blue with titanium oxide, Dyes Pigments 72 (2007) 353–356.
[4] M.A. Behnajady, N. Modirshhla, N. Daneshvar, M. Rabbani, Photocatalytic degradation of an azo dye in a tubular continuous-flow photoreactor with immobilized TiO_2 on glass plates, Chem. Eng. J. 127 (2007) 167–176.
[5] B. Neppolian, H.C. Choi, S. Sakthivel, B. Arabindoo, V. Murugesan, Comparison of the adsorption characteristics of azo-reactive dyes on mezoporous minerals, J. Hazard. Mater. 89 (2002) 303–317.
[6] N.M. Mahmoodi, M. Arami, N.Y. Limaee, N.S. Tabrizi, Kinetics of heterogeneous photocatalytic degradation of reactive dyes in an immobilized TiO_2 photocatalytic reactor, J. Colloid Interface Sci. 295 (2006) 159–164.
[7] X.Z. Li, F.B. Li, Study of Au/Au^{3+}-TiO_2 photocatalysts toward visible photooxidation for water and wastewater treatment, Environ. Sci. Technol. 35 (2001) 2381–2387.
[8] K. Erdal, I.H. Sibel, Y. Ibrahim, S. Ali, E. Oktay, Comparison of the treatment methods efficiency for decolorization mineralization of Reactive Black 5 azo dye, J. Hazard. Mater. 119 (2005) 109–116.
[9] N.M. Mahmoodi, M. Arami, Bulk phase degradation of Acid Red 14 by nanophotocatalysis using immobilized titanium(IV) oxide nanoparticles, J. Photochem. Photobiol. A 182 (2006) 60–66.
[10] S.X. Liu, X.Y. Chen, A visible light response TiO_2 photocatalyst realized by cationic S-doping and its application for phenol degradation, J. Hazard. Mater. 152 (2008) 48–55.
[11] F.B. Li, X.Z. Li, M.F. Hou, Photocatalytic degradation of 2-mercaptobenzothiazole in aqueous La^{3+}–TiO_2 suspension for odor control, Appl. Catal. B 48 (2004) 185–194.
[12] X.Z. Li, F.B. Li, C.L. Yang, W.K. Ge, Photocatalytic activity of WO_x–TiO_2 under visible light irradiation, J. Photochem. Photobiol. A 141 (2001) 209–217.
[13] M.A. Rauf, S.B. Bukallah, A. Hamadi, A. Sulaiman, F. Hammadi, The effect of operational parameters on the photoinduced decoloration of dyes using a hybrid catalyst V_2O_5/TiO_2, Chem. Eng. J. 129 (2007) 167–172.
[14] C. Koepke, K. Wisniewski, L. Sikorski, D. Piatkowski, K. Kowalska, M. Naftaly, Upconverted luminescence under 800 nm laser diode excitation in Nd^{3+}-activated fluoroaluminate glass, Opt. Mater. 28 (2006) 129–136.
[15] T. Tang, J. Zhang, B. Tian, F. Chen, D. He, M. Anpo, Preparation of Ce-TiO_2 catalysts by controlled hydrolysis of titanium alkoxide based on esterification reaction and study on its photocatalytic activity, J. Colloid Interface Sci. 315 (2007) 382–388.
[16] L. Philip, G.W. Christiane, B. Koen, Luminescent europium(III) and terbium(III) nicotinate complexes covalently linked to a 1,10-phenanthroline functionalised sol-gel glass, J. Lumin. 117 (2006) 163–169.
[17] J. Zhang, B. He, Q. Zhang, D. Huang, Photoinduced electron transfer processes of ruthenium tris(bipyridyl) and methylviologen doped in TiO_2 system by the sol-gel method, Dyes Pigments 38 (1998) 41–47.

[18] Y. Zhang, H. Zhang, Y. Xu, Y. Wang, Significant effect of lanthanide doping on the texture and properties of nanocrystalline mesoporous TiO_2, J. Solid State Chem. 177 (2004) 3490–3498.
[19] K.T. Ranjit, I. Willner, S.H. Bossmann, A.M. Braun, Lanthanide oxide-doped titanium dioxide photocatalysts: novel photocatalysts for the enhanced degradation of *p*-chlorophenoxyacetic acid, Environ. Sci. Technol. 35 (2001) 1544–1549.
[20] S. Yuan, Q. Sheng, J. Zhang, F. Cheng, M. Anpo, Q. Zhang, Synthesis of La^{3+} doped mesoporous titania with highly crystallized walls, Microporous Mesoporous Mater. 79 (2005) 93–99.
[21] Y.B. Xie, C.W. Yuan, X.Z. Li, Photocatalytic degradation of X-3B dye by visible light using lanthanide ion modified titanium dioxide hydrosol system, Colloids Surf. A 252 (2005) 87–94.
[22] P. Lu, F. Wu, N.S. Deng, Enhancement of TiO_2 photocatalytic redox ability by β-cyclodextrin in suspended solution, Appl. Catal. B 53 (2004) 87–93.
[23] F.B. Li, X.Z. Li, M.F. Hou, K.W. Cheah, W.C.H. Choy, Enhanced photocatalytic activity of Ce^{3+}-TiO_2 for 2-mercaptobenzothiazole degradation in aqueous suspension for odour control, Appl. Catal. A 285 (2005) 181–189.
[24] N.T. Abdel-Ghani, A.L. El-Ansary, A.A. Salem, Thermogravimetric, potentiometric, conductimetric and spectrometric studies on lanthanide complexes with some hydroxynaphthoic acid azo dyes, Thermochim. Acta 122 (1987) 231–243.
[25] M.F. Hou, F.B. Li, R.F. Li, H.F. Wan, G.Y. Zhou, K.C. Xie, Mechanisms of enhancement of photocatalytic properties and activity of Nd^{3+}-doped TiO_2 for methyl orange degradation, J. Rare Earths 22 (2004) 542–546.
[26] B. Yan, K. Zhou, In situ sol–gel composition of inorganic/organic polymeric hybrid precursors to synthesize red-luminescent $CaTiO_3$: Pr^{3+} and $CaTi_{0.5}Zr_{0.5}O_3$:Pr^{3+} phosphors, J. Alloys Compd. 398 (2005) 165–169.
[27] H.M. Ding, H. Sun, Y.K. Shan, Preparation and characterization of mesoporous SBA-15 supported dye-sensitized TiO_2 photocatalyst, J. Photochem. Photobiol. A-Chem. 169 (2005) 101–107.
[28] C.J. Debabrata, D. Shimanti, N.R. Nageswar, Visible light assisted photodegradation of halocarbons on the dye modified TiO_2 surface using visible light, Sol. Energy Mater. Sol. Cells 90 (2006) 1013–1020.
[29] N.T.A. Ghani, Y.M. Issa, A.A. Salem, Spectrophotometric determination of some lanthanides using 3-hydroxy-2-naphthoic acid azo dyes, Microchem. J. 39 (1989) 283–288.
[30] J.A. Navio, J.J. Testa, P. Djedjeian, J.R. Padron, D. Rodriguez, M.I. Litter, Iron-doped titania powders prepared by a sol-gel method. Part II. Photocatalytic properties, Appl. Catal. A 178 (1999) 191–203.
[31] X.Z. Li, H. Liu, L.F. Cheng, H.J. Tong, Kinetic behaviour of the adsorption and photocatalytic degradation of salicylic acid in aqueous TiO_2 microsphere suspension, J. Chem. Technol. Biotechnol. 79 (2004) 774–781.
[32] C. Mignotte, EXAFS studies on erbium-doped TiO_2 and ZrO_2 sol-gel thin films, J. Non-Cryst. Solids 291 (2001) 56–77.